New mathematical model for fluid-glucose-albumin transport in peritoneal dialysis

Roman Cherniha [1],[2] **and Jacek Waniewski** [†]

[1] *Institute of Mathematics, NAS of Ukraine,*
Tereshchenkivs'ka Street 3, 01601 Kyiv, Ukraine

[2] *Department of Mathematics, National University 'Kyiv-Mohyla Academy',*
2 Skovoroda Street, Kyiv 04070 , Ukraine
cherniha@imath.kiev.ua

[†] *Institute of Biocybernetics and Biomedical Engineering, PAS,*
Ks. Trojdena 4, 02 796 Warszawa, Poland
jacekwan@ibib.waw.pl

Abstract

A mathematical model for fluid transport in peritoneal dialysis is constructed. The model is based on a three-component nonlinear system of two-dimensional partial differential equations for fluid, glucose and albumin transport with the relevant boundary and initial conditions. Non-constant steady-state solutions of the model are studied. The restrictions on the parameters arising in the model are established with the aim to obtain exact formulae for the non-constant steady-state solutions. As the result, the exact formulae for the fluid fluxes from blood to tissue and across the tissue were constructed together with two linear autonomous ODEs for glucose and albumin concentrations. The analytical results were checked for their applicability for the description of fluid-glucose-albumin transport during peritoneal dialysis.

Keywords: fluid transport; transport in peritoneal dialysis; nonlinear partial differential equation; ordinary differential equation; steady-state solution

Mathematics Subject Classification (2010) 35K51–58, 35Q92, 92C50

1 Introduction

Peritoneal dialysis is a life saving treatment for chronic patients with end stage renal disease (Gokal R and Nolph 1994). Dialysis fluid is infused into the peritoneal cavity, and, during its dwell there, small metabolites (urea, creatinine) and other uremic toxins diffuse from blood to the fluid, and after some time (usually a few hours) are removed together with the drained fluid. The treatment is repeated continuously. The peritoneal transport occurs between dialysis fluid in the

peritoneal cavity and blood passing down capillaries in tissue surrounding the peritoneal cavity. The capillaries are distributed within the tissue at different distance from the tissue surface that is in contact with dialysis fluid. The solutes, which are transported between blood and dialysis fluid, have to cross two transport barriers: the capillary wall and a tissue layer. Typically, many solutes are transported from blood to dialysate, but some solutes that are present in high concentration in dialysis fluid are transported to blood. This kind of transport system happens also in other medical treatments, as local delivery of anticancer medications, and some experimental or natural physiological phenomena. Mathematical description of these systems was obtained using partial differential equations based on the simplification that capillaries are homogeneously distributed within the tissue (Flessner et al. 1984; Waniewski et al. 1999; Waniewski 2002). Experimental evidence confirmed the good applicability of such models (Flessner et al. 1985).

Another objective of peritoneal dialysis is to remove excess water from the patient (Gokal R and Nolph 1994). This is gained by inducing high osmotic pressure in dialysis fluid by adding a solute in high concentration. The most often used solute is glucose. This medical application of high osmotic pressure is rather unique for peritoneal dialysis. Mathematical description of fluid and solute transport between blood and dialysis fluid in the peritoneal cavity has not been formulated fully yet, in spite of the well known basic physical laws for such transport. A previous attempt did not result in a satisfactory description, and was disproved later on (Seames et al. 1990;Flessner 1994). Recent mathematical, theoretical and numerical studies introduced new concepts on peritoneal transport and yielded better results for the transport of fluid and osmotic agent (Cherniha and Waniewski 2005; Stachowska-Pietka et al. 2005; Stachowska-Pietka et al. 2006; Cherniha et al. 2007;Waniewski et al.2007, Waniewski et al.2009). However, the problem of a combined description of osmotic ultrafiltration to the peritoneal cavity, absorption of osmotic agent from the peritoneal cavity and leak of macromolecules (proteins, e.g., albumin) from blood to the peritoneal cavity has not been addressed yet, see for example in (Flessner 2001; Stachowska-Pietka et al. 2007). Therefore, we present here a new extended model for these phenomena and investigate its mathematical structure.

The paper is organized as follows. In section 2, a mathematical model of glucose and albumin transport in peritoneal dialysis is constructed. In section 3, non-constant steady-state solutions of the model are constructed and their properties are investigated. Moreover, these solutions are tested for the real parameters that represent clinical treatments of peritoneal dialysis. The results are compared with those derived by numerical simulations for a simplified model (Cherniha et al. 2007).

Finally, we present some conclusions and discussion in the last section.

2. Mathematical model

The mathematical description of transport processes within the tissue consists in local balance of fluid volume and solute mass. For incompressible fluid, the change of volume may occur due to elasticity of the tissue. The fractional void volume, i.e. the volume occupied by the fluid in the interstitium (the rest of the tissue being cells and macromolecules forming interstitium) expressed per one unit volume of the whole tissue is denoted $\nu(t,x)$, and its time evolution is described by the following equation:

$$\frac{\partial \nu}{\partial t} = -\frac{\partial j_U}{\partial x} + q_U - q_l \tag{1}$$

where $j_U(t,x)$ is the volumetric fluid flux across the tissue (ultrafiltration), $q_U(t,x)$ is the density of volumetric fluid flux from blood to the tissue, while the density of volumetric fluid flux from the tissue to the lymphatic vessels q_l (hereafter we assume that it is a known positive constant, nevertheless it can be also a function of hydrostatic pressure) produces absorbtion of solutes from the tissue.

The independent variables t is time, and x is the distance from the tissue surface in contact with dialysis fluid (flat geometry of the tissue is here assumed). The solutes, glucose and albumin, are distributed only within the interstitial fluid, and their concentrations in this fluid are denoted by $C_G(t,x)$ and $C_A(t,x)$, respectively. The equation that describes the local changes of glucose amount, νC_G, is as follows:

$$\frac{\partial(\nu C_G)}{\partial t} = -\frac{\partial j_G}{\partial x} + q_G, \tag{2}$$

where $j_G(t,x)$ is glucose flux through the tissue, and $q_G(t,x)$ is the density of glucose flux from blood.

Similarly, equation that describes the local changes of albumin amount, νC_A, is as follows:

$$\frac{\partial(\alpha\nu C_A)}{\partial t} = -\frac{\partial j_A}{\partial x} + q_A, \tag{3}$$

where $j_A(t,x)$ is albumin flux through the tissue, and $q_A(t,x)$ is the density of albumin flux from blood, while the coefficient $\alpha < 1$ takes into account that a part of the fractional void volume ν is only accessible for albumin because of big size of molecules (Flessner 2001; Stachowska-Pietka et al. 2007). The flows of fluid and solutes are described according to linear non-equilibrium thermodynamics. Osmotic pressure of glucose and oncotic pressure of albumin are described by van't Hoff law, i.e. it is proportional to the relevant concentrations.

The fluid flux across the tissue is generated by hydrostatic, osmotic and oncotic pressure gradients:

$$j_U = -\nu K \frac{\partial P}{\partial x} + \sigma_{TG} \nu K R T \frac{\partial C_G}{\partial x} + \sigma_{TA} \gamma \nu K R T \frac{\partial C_A}{\partial x}, \tag{4}$$

whereas for the density of fluid flux from blood to tissue we assume that it is generated by the hydrostatic, osmotic and oncotic pressure differences between blood and tissue:

$$q_U = L_p a (P_B - P) - L_p a \sigma_G R T (C_{GB} - C_G) - \gamma L_p a \sigma_A R T (C_{AB} - C_A), \tag{5}$$

where $P(t, x)$ is hydrostatic pressure.

The glucose solute flux across the tissue is composed of diffusive component (proportional to glucose concentration gradient) and convective component (proportional to glucose concentration and fluid flux):

$$j_G = -\nu D_G \frac{\partial C_G}{\partial x} + S_{TG} C_G j_U. \tag{6}$$

The density of glucose flux from blood to tissue has diffusive component (proportional to the difference of glucose concentration in blood, C_{GB}, and glucose concentration in tissue, C_G), convective component (proportional to the density of fluid flow from blood to tissue, q_U) and component presenting lymphatic absorbtion:

$$q_G = p_G a (C_{GB} - C_G) + S_G q_U \left((1 - F_G) C_{GB} + F_G C_G\right) - q_l C_G. \tag{7}$$

In quite similar way, we can construct equations for the albumin solute flux across the tissue,$j_A(t, x)$, and the density of albumin flux from blood to tissue $q_A(t, x)$:

$$j_A = -\alpha \nu D_A \frac{\partial C_A}{\partial x} + S_{TA} C_A j_U, \tag{8}$$

$$q_A = p_A a (C_{AB} - C_A) + S_A q_U \left((1 - F_A) C_{AB} + F_A C_A\right) - q_l C_A. \tag{9}$$

The coefficients in the above equations are: K – hydraulic permeability of tissue, σ_{TG} and σ_{TA} – the Staverman reflection coefficients for glucose and albumin in tissue, $S_{TG} = 1 - \sigma_{TG}$ and $S_{TA} = 1 - \sigma_{TA}$– sieving coefficients of glucose and albumin in tissue, σ_G and σ_A – the Staverman reflection coefficients for glucose and albumin in the capillary wall, $S_G = 1 - \sigma_G$ and $S_A = 1 - \sigma_A$– sieving coefficients of glucose and albumin in the capillary wall, R – gas constant, T – temperature, L_p – hydraulic permeability of the capillary wall, a – density of capillary surface area, D_G and D_A – diffusivities of glucose and albumin in tissue, p_G and p_A – diffusive permeabilities

of the capillary wall for glucose and albumin, P_B - hydrostatic pressure in blood, $F_G \leq 1$ and $F_A \leq 1$ – weighing factors, and $\gamma \leq 1$ is a coefficient that recalculates osmotic pressure of albumin to the total oncotic pressure exerted by all proteins (Stachowska-Pietka et al. 2007).

Equations (1)-(3) together with equations (4)-(9) for flows form a system of three nonlinear partial differential equations with three variables: ν, P, C_A, and C_G. Therefore, an additional, constitutive, equation is necessary, and this is the equation describing how fractional fluid volume, ν, depends on interstitial pressure, P. This dependence can be established using data from experimental studies (Stachowska-Pietka et al. 2006). It turns out that

$$\nu = F(P), \tag{10}$$

where F is a monotonically non-decreasing bounded function with the limits: $F \to \nu_{\min}$ if $P \to P_{\min}$ and $F \to \nu_{\max}$ if $P \to P_{\max}$ (particularly, one may take $P_{\min} = -\infty,\ P_{\max} = \infty$). Here $\nu_{\min} < 1$ and $\nu_{max} < 1$ are empirically measured constants. The reader may find possible analytical forms for the function F in (Stachowska-Pietka et al. 2006; Cherniha et al. 2007).

Boundary conditions for a tissue layer of width L impermeable at $x = L$ and in contact with dialysis fluid at $x = 0$ are as follows:

$$x = 0: \ P = P_D, \quad C_G = C_{GD}, \quad C_A = C_{AD} \tag{11}$$

$$x = L: \ \frac{\partial P}{\partial x} = 0, \quad \frac{\partial C_G}{\partial x} = 0, \quad \frac{\partial C_A}{\partial x} = 0. \tag{12}$$

Initial conditions describe equilibrium within the tissue without any contact with dialysis fluid at $x = 0$:

$$t = 0: \ P = P_0, \ C_G = C_{GB}, \ C_A = C_{AB}. \tag{13}$$

It is easily seen that equations (1)-(10) can be united into three nonlinear partial differential equations (PDEs) for finding the hydrostatic pressure $P(t, x)$, the glucose concentration C_G and the albumin concentration C_A. Thus, these PDEs together with boundary and initial conditions (11)-(13) form the nonlinear boundary-value problem. Possible values of the parameters arising in this problem can be established from experimental data published in a wide range of papers.

Finally, we note that finding the function $j_U(t, x)$, presenting the fluid fluid flux across the tissue and calculating ultrafiltration from the tissue to peritoneal cavity, is the most important.

3. Steady-state solutions of the model and their applications

First of all we consider the special case: if the boundary conditions (11) is replaced by zero Neumann conditions at $x = 0$ then the steady state solution can be easily found because it does't depend on x. In fact solving algebraic equations

$$q_U - q_l = 0, \quad q_G = 0, \quad q_A = 0, \tag{14}$$

one easily obtains the constant steady-state solution

$$\begin{aligned} C_G^* &= \tfrac{p_G a + q_l S_G(1-F_G)}{p_G a + q_l(1-S_G F_G)} C_{GB} \\ C_A^* &= \tfrac{p_A a + q_l S_A(1-F_A)}{p_A a + q_l(1-S_A F_A)} C_{AB} \\ P^* &= P_B - q_l\Big(\tfrac{1}{L_p a} + RT\Big(\tfrac{\sigma_G^2}{p_G a + q_l(1-S_G F_G)} + \tfrac{\gamma\sigma_A^2}{p_A a + q_l(1-S_A F_A)}\Big)\Big). \end{aligned} \tag{15}$$

In the case $q_l = 0$, i.e., zero flux from the tissue to the lymphatic vessels, formulae (15) produce

$$C_G^* = C_{GB}, \quad C_A^* = C_{AB}, \quad P^* = P_B, \tag{16}$$

otherwise

$$C_G^* < C_{GB}, \quad C_A^* < C_{AB}, \quad P^* < P_B. \tag{17}$$

However, such solution cannot describe any peritoneal transport.

To find non-constant steady-state solutions, we reduce Eqs. (1)-(3) to an equivalent form by introducing non-dimensional independent and dependent variables

$$x^* = \frac{x}{L}, \quad t^* = \frac{K(P_D - P_0)t}{L^2}, \tag{18}$$

$$p(t^*, x^*) = \frac{P - P_0}{P_D - P_0}, \quad u(t^*, x^*) = \frac{C_G - C_{GB}}{C_{GD} - G_{GB}}, \quad w(t^*, x^*) = \frac{C_A}{C_{GD} - G_{GB}}. \tag{19}$$

Thus, after rather simple calculations and taking into account Eq. (4), (6), and (8), one obtains Eq. (1)-(3) in the forms (hereafter upper index $*$ is omitted)

$$\frac{1}{t_0}\frac{\partial \nu}{\partial t} = \frac{1}{t_0}\frac{\partial}{\partial x}\Big(\frac{\nu \partial p}{\partial x}\Big) - \sigma_1\frac{\partial}{\partial x}\Big(\frac{\nu \partial u}{\partial x}\Big) - \sigma_2\frac{\partial}{\partial x}\Big(\frac{\nu \partial w}{\partial x}\Big) + q_U - q_l, \tag{20}$$

$$\begin{aligned} &\frac{1}{t_0}\frac{\partial(\nu u)}{\partial t} + \frac{\sigma_{TG}u_0}{t_0}\frac{\partial \nu}{\partial t} = d_1\frac{\partial}{\partial x}\Big(\frac{\nu \partial u}{\partial x}\Big) + \frac{S_{TG}}{t_0}\frac{\partial}{\partial x}\Big(\frac{u\nu \partial p}{\partial x}\Big) - S_{TG}\sigma_1\frac{\partial}{\partial x}\Big(\frac{u\nu \partial u}{\partial x}\Big) \\ &-S_{TG}\sigma_2\frac{\partial}{\partial x}\Big(\frac{u\nu \partial w}{\partial x}\Big) + (u_0(S_G - S_{TG}) + S_G F_G u)q_U - b_1 u - \sigma_{TG}u_0 q_l, \end{aligned} \tag{21}$$

$$\frac{1}{t_0}\frac{\partial(\nu w^*)}{\partial t}+\frac{\sigma_{TA}w_0}{t_0}\frac{\partial \nu}{\partial t}=d_2\frac{\partial}{\partial x}\Big(\frac{\nu\partial w}{\partial x}\Big)+\frac{S_{TA}}{t_0}\frac{\partial}{\partial x}\Big(\frac{w^*\nu\partial p}{\partial x}\Big)-S_{TA}\sigma_1\frac{\partial}{\partial x}\Big(\frac{w^*\nu\partial u}{\partial x}\Big)$$

$$-S_{TA}\sigma_2\frac{\partial}{\partial x}\Big(\frac{w^*\nu\partial w}{\partial x}\Big)+(w_0(S_A-S_{TA})+S_AF_Aw^*)q_U-b_2w^*-\sigma_{TA}w_0q_l, \quad (22)$$

where

$$\begin{aligned}
&q_U=\tfrac{L_paL^2}{K}\Big(\tfrac{1}{t_0}(p_0-p)+\tfrac{\sigma_G\sigma_1}{\sigma_{TG}}u+\tfrac{\sigma_A\sigma_2}{\sigma_{TA}}w^*\Big),\\
&\sigma_1=\sigma_{TG}KRT\tfrac{C_{GD}-G_{GB}}{L^2}, \quad \sigma_2=\sigma_{TA}KRT\gamma\tfrac{C_{GD}-G_{GB}}{L^2},\\
&d_1=\tfrac{D_G}{L^2}, \quad d_2=\tfrac{\alpha D_A}{L^2},\\
&b_1=p_Ga+q_l, \quad b_2=p_Aa+q_l,\\
&u_0=\tfrac{C_{GB}}{C_{GD}-G_{GB}}, \quad w_0=\tfrac{C_{AB}}{C_{GD}-G_{GB}}, \quad p_0=\tfrac{P_B-P_0}{P_D-P_0}\\
&t_0=\tfrac{L^2}{K(P_D-P_0)}, \quad w^*=w-w_0,
\end{aligned} \quad (23)$$

We want to find the steady state solutions of Eqs. (20)-(22) satisfying the boundary conditions (11)-(12). They take the form

$$x=0:\ p=1, \quad u=1, \quad w=\frac{C_{AD}}{C_{GD}-G_{GB}} \quad (24)$$

$$x=1:\ \frac{\partial p}{\partial x}=0, \quad \frac{\partial u}{\partial x}=0, \quad \frac{\partial w}{\partial x}=0. \quad (25)$$

for the non-dimensional variables.

Obviously, Eqs. (20)-(22) can be reduced to the ordinary differential equations (ODEs) to find steady state solutions:

$$\frac{1}{t_0}\frac{d}{dx}\Big(\frac{\nu dp}{dx}\Big)-\sigma_1\frac{d}{dx}\Big(\frac{\nu du}{dx}\Big)-\sigma_2\frac{d}{dx}\Big(\frac{\nu dw}{dx}\Big)+q_U-q_l=0, \quad (26)$$

$$d_1\frac{d}{dx}\Big(\frac{\nu du}{dx}\Big)+\frac{S_{TG}}{t_0}\frac{d}{dx}\Big(\frac{u\nu dp}{dx}\Big)-S_{TG}\sigma_1\frac{d}{dx}\Big(\frac{u\nu du}{dx}\Big)$$

$$-S_{TG}\sigma_2\frac{d}{dx}\Big(\frac{u\nu dw}{dx}\Big)+(u_0(S_G-S_{TG})+S_GF_Gu)q_U-b_1u-\sigma_{TG}u_0q_l=0, \quad (27)$$

$$d_2\frac{d}{dx}\Big(\frac{\nu dw}{dx}\Big)+\frac{S_{TA}}{t_0}\frac{d}{dx}\Big(\frac{w^*\nu dp}{dx}\Big)-S_{TA}\sigma_1\frac{d}{dx}\Big(\frac{w^*\nu du}{dx}\Big)$$

$$-S_{TA}\sigma_2\frac{d}{dx}\Big(\frac{w^*\nu dw}{dx}\Big)+(w_0(S_A-S_{TA})+S_AF_Aw^*)q_U-b_2w^*-\sigma_{TA}w_0q_l=0. \quad (28)$$

Non-linear system of ODEs (26)-(28) is still very complicated for integrations with arbitrary coefficients. Thus, we look for the correctly-specified coefficients when this system can be simplified. It can be noted that the relations

$$S_A = S_{TA}, \quad S_G = S_{TG} \tag{29}$$

lead to an essential simplification of this system. In fact, using equation (26), expressions for q_U from (23) and j_U from (4), rewritten in non-dimensional variables

$$j_U = L\nu\Big(-\frac{1}{t_0}\frac{\partial p}{\partial x} + \sigma_1\frac{\partial u}{\partial x} + \sigma_2\frac{\partial w}{\partial x}\Big), \tag{30}$$

one arrives at the semicoupled system of ODEs

$$\frac{K}{L_p a L^2}\frac{d}{dx}\Big(\frac{\nu dq_U}{dx}\Big) = q_U - q_l \tag{31}$$

$$j_U = \frac{K\nu}{L_p a L}\frac{dq_U}{dx} \tag{32}$$

to find functions q_U and j_U.

Equation (31) is the linear second-order ODE provided the function ν is known. Nevertheless ν depends on the pressure, which is also to be found function, we may use additional restrictions on the given function F from (10). For example, assuming that F is proportional to the inverse function to $P(x)$, we obtain

$$\nu(x) = \nu_m, \tag{33}$$

where ν_m is a positive constant. Substituting (33) into system (31)–(32), we easily find its general solution:

$$q_U = C_1 e^{-\lambda x} + C_2 e^{\lambda x} + q_l, \tag{34}$$

$$j_U = \frac{L}{\lambda}(-C_1 e^{-\lambda x} + C_2 e^{\lambda x}), \quad \lambda = \sqrt{\frac{L_p a L^2}{K\nu_m}}. \tag{35}$$

The arbitrary constants C_1 and C_2 can be specified using the boundary conditions (24)–(25) since the functions q_U and j_U are expressed via $p,\ u,\ w$ and their first-order derivatives (see formulae (23) and (30)). Making rather simple calculations, one obtains

$$C_1 = (q_0 - q_l)\frac{e^{2\lambda}}{1+e^{2\lambda}}, \quad C_2 = (q_0 - q_l)\frac{1}{1+e^{2\lambda}}, \tag{36}$$

where

$$q_0 = \frac{L_p a L^2}{K}\Big(\frac{1}{t_0}(p_0 - 1) + \sigma_1 + \sigma_2\frac{C_{AD} - C_{AB}}{C_{GD} - G_{GB}}\Big). \tag{37}$$

Having the explicit formulae for q_U and j_U, system of ODEs (27) and (28) with restrictions (29) can be reduced to two linear autonomous ODEs

$$d_1\nu_m\frac{d^2u}{dx^2} + \frac{S_G}{\lambda}(C_1e^{-\lambda x} - C_2e^{\lambda x})\frac{du}{dx} + \Big(f_1(C_1e^{-\lambda x} + C_2e^{\lambda x}) - \kappa_1\Big)u - u_{01} = 0 \tag{38}$$

and

$$d_2\nu_m\frac{d^2w}{dx^2} + \frac{S_A}{\lambda}(C_1e^{-\lambda x} - C_2e^{\lambda x})\frac{dw}{dx} + \Big(f_2(C_1e^{-\lambda x} + C_2e^{\lambda x}) - \kappa_2\Big)(w - w_0) - w_{01} = 0 \tag{39}$$

to find the functions $u(x)$ and $w(x)$. Hereafter the notations

$$\begin{array}{lll} f_1 = S_GF_G - S_G, & \kappa_1 = p_Ga + (1 - S_GF_G)q_l, & u_{01} = \sigma_Gu_0q_l, \\ f_2 = S_AF_A - S_A, & \kappa_2 = p_Aa + (1 - S_AF_A)q_l, & w_{01} = \sigma_Aw_0q_l \end{array} \tag{40}$$

are used. To our best knowledge, the general solutions of ODEs (38) and (39) (obviously, both equations have the same structure) are unknown in explicit form. On the other hand, since the unknown functions $u(x)$ and $w(x)$ should satisfy the boundary conditions (24)–(25), the corresponding linear problems can be numerically solved using, for example, Maple program package. Finally, using two expressions for q_U from (23) and (34), we obtain the function

$$p(x) = p_0 + t_0\sigma_1u + t_0\sigma_2(w - w_0) - \frac{t_0K}{L_paL^2}\Big(C_1e^{-\lambda x} + C_2e^{\lambda x} - q_l\Big). \tag{41}$$

In the next section, the realistic values of parameters arising in the formulae derived above will be established and used to calculate the steady-state solutions of the model with restrictions (29) and (33).

Since restriction (33) is rather an artificial simplification for modeling fluid transport in peritoneal dialysis and it needs additional justifications, we examined the cases when the function ν is non-constant and satisfies the properties presented after formula (10). The simplest case occurs when ν is linear monotonically decreasing function

$$\nu(p(x)) \equiv \nu(x) = \nu_{max} - (\nu_{max} - \nu_{min})x, \quad x \in [0, 1]. \tag{42}$$

Substituting (42) into (29), we obtain the linear ODE

$$(\nu_{max} - (\nu_{max} - \nu_{min})x)\frac{d^2q_U}{dx^2} - (\nu_{max} - \nu_{min})\frac{dq_U}{dx} - \frac{L_paL^2}{K}(q_U - q_l) = 0. \tag{43}$$

It turns out that this ODE reduces to the modified Bessel equation of the zero order (see, e.g., Bateman 1974)

$$y^2\frac{d^2q_V}{dy^2}+y\frac{dq_V}{dy}-y^2q_V=0 \tag{44}$$

by the substitution

$$y^2=4\delta_*(\nu_*-x),\ q_V=q_U-q_l,\ \nu_*=\frac{\nu_{max}}{\nu_{max}-\nu_{min}}>1,\ \delta_*=\frac{L_paL^2}{K(\nu_{max}-\nu_{min})}>0 \tag{45}$$

The general solution of (44) is well-known, hence, using formulae (45), one obtains the solution of (43):

$$q_U=C_1I_0(2\sqrt{\delta_*(\nu_*-x)})+C_2K_0(2\sqrt{\delta_*(\nu_*-x)})+q_l, \tag{46}$$

where I_0 and K_0 are the modified Bessel functions of the first and third kind, respectively.

Substituting the function q_U obtained into (31) and using the well-known relations between the Bessel functions (Bateman 1974), we find the function:

$$j_U=-L\sqrt{\frac{\nu_*-x}{\delta_*}}\Big(C_1I_1(2\sqrt{\delta_*(\nu_*-x)})-C_2K_1(2\sqrt{\delta_*(\nu_*-x)})\Big), \tag{47}$$

where I_1 and K_1 are the modified Bessel functions of the first order. The arbitrary constants C_1 and C_2 can be specified in the quite similar way as this was done in the case $\nu(x)=const$. Omitting rather simple calculations, we present only the result:

$$C_1=\frac{(q_0-q_l)K_1(2\sqrt{\delta_*(\nu_*-1)})}{I_0(2\sqrt{\delta_*\nu_*})K_1(2\sqrt{\delta_*(\nu_*-1)})+K_0(2\sqrt{\delta_*\nu_*})I_1(2\sqrt{\delta_*(\nu_*-1)})}, \tag{48}$$

$$C_2=\frac{(q_0-q_l)I_1(2\sqrt{\delta_*(\nu_*-1)})}{I_0(2\sqrt{\delta_*\nu_*})K_1(2\sqrt{\delta_*(\nu_*-1)})+K_0(2\sqrt{\delta_*\nu_*})I_1(2\sqrt{\delta_*(\nu_*-1)})}, \tag{49}$$

where q_0 is defined by (37).

Thus, we have found the explicit formulae for q_U and j_U. In contrast to the case $\nu(x)=const$, they contain not only elementary functions but transcendental functions as well. Having formulae (46)–(47), system of ODEs (27) and (28) with restrictions (29) can be reduced to two linear autonomous ODEs to find the functions $u(x)$ and $w(x)$. These equations possess the forms

$$\begin{aligned}&d_1(\nu_{max}-\nu_{min})\Big((\nu_*-x)\tfrac{d^2u}{dx^2}-\tfrac{du}{dx}\Big)\\&-\tfrac{S_G}{\sqrt{\delta_*}}\tfrac{d}{dx}\Big(\sqrt{\nu_*-x}(C_1I_1(2\sqrt{\delta_*(\nu_*-x)})-C_2K_1(2\sqrt{\delta_*(\nu_*-x)}))u\Big)\\&+\Big(S_GF_G(C_1I_0(2\sqrt{\delta_*(\nu_*-x)})+C_2K_0(2\sqrt{\delta_*(\nu_*-x)}))-\kappa_1\Big)u-u_{01}=0\end{aligned} \tag{50}$$

and

$$
\begin{aligned}
&d_2(\nu_{max}-\nu_{min})\Big((\nu_*-x)\tfrac{d^2w}{dx^2}-\tfrac{dw}{dx}\Big)\\
&-\tfrac{S_A}{\sqrt{\delta_*}}\tfrac{d}{dx}\Big(\sqrt{\nu_*-x}(C_1I_1(2\sqrt{\delta_*(\nu_*-x)})-C_2K_1(2\sqrt{\delta_*(\nu_*-x)}))(w-w_0)\Big)\\
&+\Big(S_AF_A(C_1I_0(2\sqrt{\delta_*(\nu_*-x)})+C_2K_0(2\sqrt{\delta_*(\nu_*-x)}))-\kappa_2\Big)(w-w_0)-w_{01}=0
\end{aligned}
\tag{51}
$$

Nevertheless both equations are linear second order ODEs with the same structure, it seems to be unrealistic to construct their general solutions because of their awkwardness. Thus, we will numerically solve them together with the boundary conditions (24)–(25), using Maple program package. In the next section, the realistic values of the parameters arising in formulae (46)–(51) will be established and used to calculate the steady-state solutions.

4. Applications for the peritoneal transport

Here we present the results of application of the formulae derived in Section 3. Our aim is to check whether they are applicable for describing the fluid-glucose-albumin transport in peritoneal dialysis. The parameters arising in the formulae were derived from experimental data and applied in previous mathematical studies (Imholz et al. 1998; Zakaria et al. 1999; Flessner 2001; Waniewski 2001; Waniewski 2004; Stachowska-Pietka et al. 2006; Cherniha et al. 2007).

Thus, we used the following values of parameters and absolute constants: $K = 5.14{\cdot}10^{-5}\ cm^2{\cdot}min^{-1}{\cdot}mmHg^{-1}$ - hydraulic permeability of tissue, $RT = 18{\cdot}10^3\ mmHg\cdot mmol^{-1}\cdot mL$ - gas constant times temperature, $L = 1.0\ cm$ - width of the tissue layer, $L_Pa = 7.3\cdot 10^{-5}\ mL\cdot min^{-1}\cdot mmHg^{-1}\cdot g^{-1}$- hydraulic permeability of the capillary wall, $q_l = 0.26\cdot 10^{-4}\ mL\cdot min^{-1}\cdot cm^{-3}$ - volumetric fluid flux from the tissue to the lymphatic vessels, $D_G = 12.11\cdot 10^{-5}\ cm^2\cdot min^{-1}$ - diffusivity of glucose in tissue divided by ν_0, $D_A = 0.2\cdot 10^{-5}\ cm^2\cdot min^{-1}$ - diffusivity of albumin in tissue divided by ν_0, $p_Ga = 3.4{\cdot}10^{-2}\ mL{\cdot}min^{-1}{\cdot}g^{-1}$ - diffusive permeability of the capillary wall for glucose, $p_Aa = 3{\cdot}10^{-4}\ mL{\cdot}min^{-1}{\cdot}g^{-1}$ - diffusive permeability of the capillary wall for albumin (there are no precise values for this parameter in literature, however, p_A is expected to be at least 100 times smaller than p_G [13]), σ_{TG} - the Staverman reflection coefficient for glucose in tissue (varies from 0 to 0.01), $S_{TG} = 1-\sigma_{TG}$ - sieving coefficient of glucose in tissue, σ_{TA} - the Staverman reflection coefficient for albumin in tissue (varies from 0.05 to 0.5), $S_{TA} = 1-\sigma_{TA}$ - sieving coefficient of albumin in tissue, $C_{GB} = 6\cdot 10^{-3}\ mmol\cdot mL^{-1}$ and $C_{AB} = 0.6\cdot 10^{-3}\ mmol\cdot mL^{-1}$- glucose and albumin concentration in the blood, respectively, $C_{GD} = 180\cdot 10^{-3}\ mmol\cdot mL^{-1}$ and $C_{AD} = 0$ - glucose and albumin concentration in the dialysate,

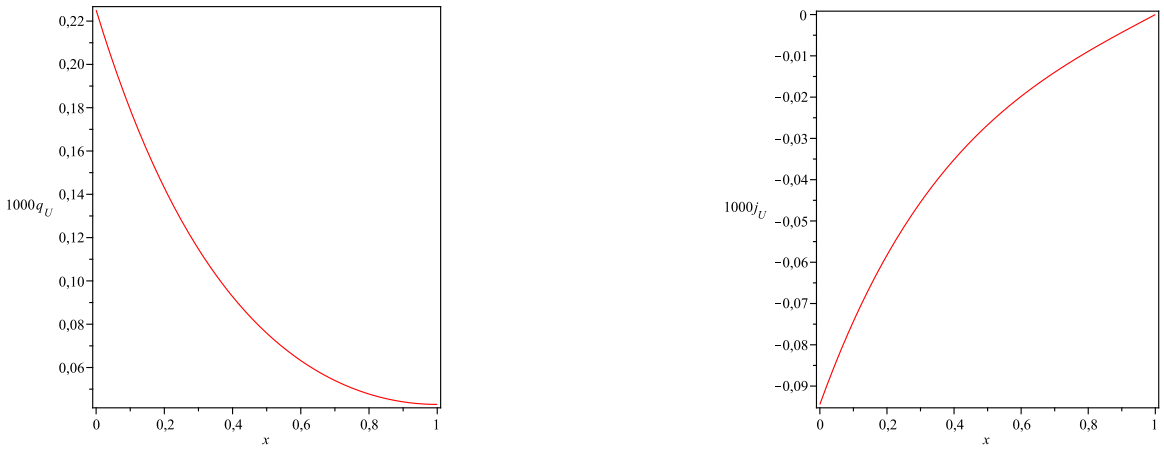

Figure 1: The fluid flux from blood to tissue q_U (in $mL \cdot min^{-1} \cdot cm^{-3}$) and the fluid flux across tissue j_U (in $mL \cdot min^{-1} \cdot cm^{-2}$) in the case $\nu = (\nu_{max} + \nu_{min})/2 = 0.26$, $\sigma_{TG} = 0.001$, and $\sigma_{TA} = 0.25$.

respectively, $P_B = 15\ mmHg$ - hydrostatic pressure in the blood, $P_D = 12\ mmHg$ - intraperitoneal hydrostatic pressure, $P_0 = 0$ - initial interstitial hydrostatic pressure, $F_G = 0.5$ and $F_A = 0.5$ – weighing factors for glucose and albumin, respectively, and the non-dimensional coefficients $\nu_{\min} = 0.17, \nu_{max} = 0.35, \nu_0 = 0.17$, $\alpha = 0.8, \gamma = 1$.

Let us consider the first case, when restrictions (29) and (33) take place. First of all, it seems to be reasonable to set $\nu_m = (\nu_{max} + \nu_{min})/2 = 0.26$, i.e., we assume that the fractional void volume at the steady state stage of the the peritoneal transport is an intermediate value between its maximum and minimum. The Staverman reflection coefficients for glucose and albumin in tissue are now $\sigma_{TG} = 0.001$ and $\sigma_{TA} = 0.25$, respectively.

Fig.1 presents the space distributions of the density of fluid flux from blood to tissue q_U and the fluid flux across tissue j_U, calculated using formulae (34)–(37). One sees that the function $q_U(x)$ is monotonically decreasing, while the function $j_U(x)$ is monotonically increasing with the distance from the peritoneal surface, and this corresponds to the experimental data and numerical simulations for the simplified model (Cherniha et al. 2007; Waniewski et al. 2007).

Using the value of the fluid flux j_U at the point $x = 0$, one may calculate the reverse water flow (i.e. out of the tissue to the cavity). Total fluid outflow from the tissue to the cavity, calculated assuming that the surface area of the contact between dialysis fluid and peritoneum is equal to 0.5 m^2, is about 0.50 mL/min. Note the similar value was obtained in (Cherniha et al. 2007) using numerical simulations for the simplified model.

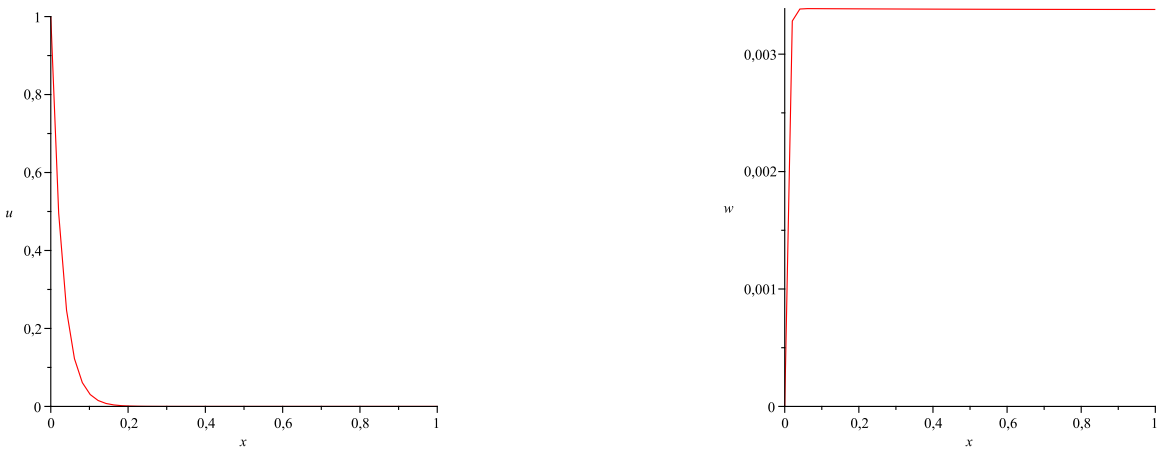

Figure 2: The non-dimensional glucose concentration u and albumin concentration w in the case $\nu = (\nu_{max} + \nu_{min})/2 = 0.26$, $\sigma_{TG} = 0.001$, $\sigma_{TA} = 0.25$, and $p_A a = 3 \cdot 10^{-4}$ $mL \cdot min^{-1} \cdot g^{-1}$.

Fig.2 presents the space distributions of the glucose and albumin concentrations. The glucose concentration u decreases rapidly with the distance from the peritoneal cavity to zero in the deeper tissue layer and is practically zero for $x > 0.15$. As one may expect, the albumin concentration w increases with the distance from the peritoneal cavity. However, the concentration increases rapidly only in a very thin layer, while for any $x > 0.05$ it is practically constant, $w \simeq 0.0034$, and in agreement with the initial albumin profile $C_A = C_{AB} = 0.6 \cdot 10^{-3}$ $mmol \cdot mL^{-1}$ (see (13)). However, such sharp increase in concentration is rather unrealistic and is a consequence of the assumption (33).

Let us consider now the second case, which is more realistic. We assume that restrictions (29) and (42) take place. The Staverman reflection coefficients were chosen the same as in the first case, i.e., $\sigma_{TG} = 0.001$ and $\sigma_{TA} = 0.25$. The results are presented on Fig. 3 and 4. It is quite interesting that the profiles for the functions $q_U(x)$ and $j_U(x)$ pictured on Fig.3 are very similar to those on Fig. 1, although the relevant formulae are essentially different (the reader may compare (46) – (49) with (34)–(37)). Moreover, the total fluid outflow from the tissue to the cavity, calculated under the above mentioned assumption is approximately equal to -0.55 mL/min, that is only about 10 percents higher than in the previous case.

The space distributions of the glucose and albumin concentrations are pictured on Fig.4. The glucose concentration u is again a decreasing function, however the tissue layer with non-vanishing u is wider.

The main difference occurs in the case of the albumin concentration w. We

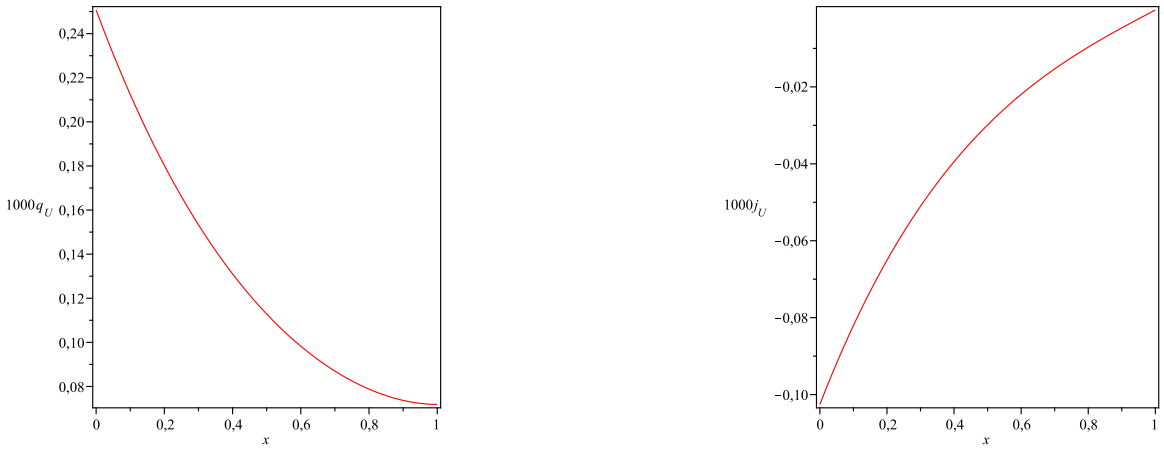

Figure 3: The fluid flux from blood to tissue q_U (in $mL \cdot min^{-1} \cdot cm^{-3}$) and the fluid flux across tissue j_U (in $mL \cdot min^{-1} \cdot cm^{-2}$) in the case $\nu = \nu_{max} - (\nu_{max} - \nu_{min})x$, $\sigma_{TG} = 0.001$, and $\sigma_{TA} = 0.25$.

found that the albumin concentration w essentially depends on the parameter $p_A a$. Three curves pictured on Fig.4 correspond to the values of the diffusive permeability $p_A a = 5 \cdot 10^{-4}$, $3 \cdot 10^{-4}$, and $2 \cdot 10^{-4}$ $mL \cdot min^{-1} \cdot g^{-1}$, respectively. Negative values occurring close to the peritoneal cavity (the red curve corresponding to the smallest $p_A a$ value) are very small and can be either a consequence of the simplifications in the model or an error in numerical solving ODE (51). We may interpret these negative values as follows: there is no albumin in this layer of the tissue because it was already removed to the peritoneal cavity.

Finally, one observes that the relevant curves on Fig.2 and Fig.4 (the middle curve) are essentially different, nevertheless they were obtained for the same parameters. As follows from the Fig.4, the albumin concentration w increases in deeper layers of tissue as well, and is equal to the constant, corresponding to the initial profile, only close to the opposite side of tissue. Thus, such steady-state profile of the albumin concentration is more realistic than in the first case (see Fig.2).

5. Conclusions

In this paper, a new mathematical model for fluid transport in peritoneal dialysis was constructed. The model is based on a three-component nonlinear system of two-dimensional partial differential equations and the relevant boundary and initial conditions. To analyze the non-constant steady-state solutions, the model was reduced to the non-dimensional form. Having in mind to obtain exact formulae for such solutions, we found the restrictions on parameters arising in the model that essentially simplified the equations of the model. As the result, the exact formulae

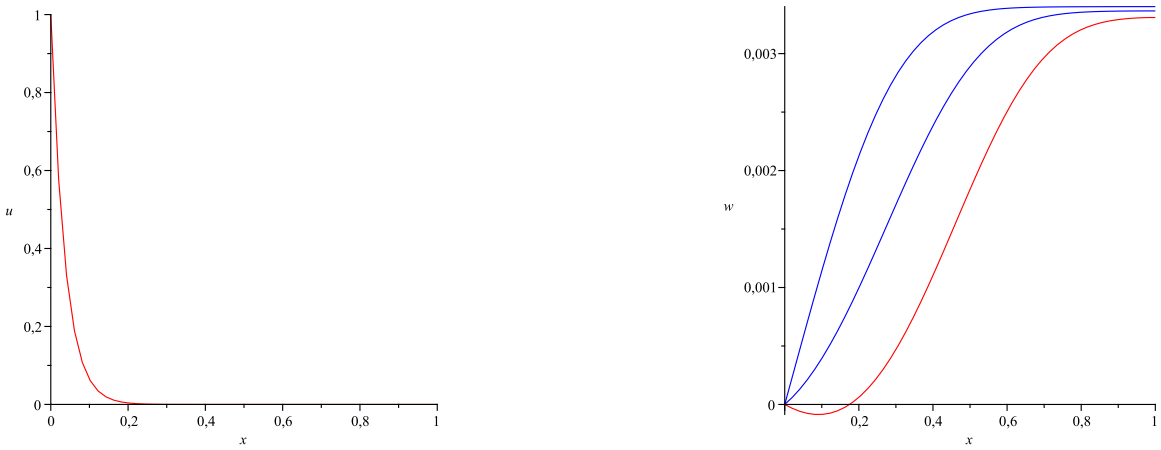

Figure 4: The non-dimensional glucose concentration u and albumin concentration w in the case $\nu = \nu_{max} - (\nu_{max} - \nu_{min})x$, $\sigma_{TG} = 0.001$, $\sigma_{TA} = 0.25$, and $p_A a = 5 \cdot 10^{-4}$, $3 \cdot 10^{-4}$, $2 \cdot 10^{-4}$ $mL \cdot min^{-1} \cdot g^{-1}$

for the density of fluid flux from blood to tissue and the fluid flux across the tissue were constructed together with two linear autonomous ODEs for glucose and albumin concentrations.

The analytical results were checked, whether they are applicable for describing the fluid-glucose-albumin transport in peritoneal dialysis. Thus, the realistic values of the parameters, arising in the formulae, were used to calculate the steady-state solutions of the model. The conclusion is rather optimistic because even the simplest approximation of fractional fluid volume ν via linear function with the correctly specified coefficients leads to plausible results. Other, more realistic approximation of ν may in future result in similar exact formulae. However, in general the assumption about equality of the reflection coefficients in the tissue and in the capillary wall, although it demonstrates an interesting specific symmetry in the equations, can be too restrictive for practical applications of the derived formulae (Waniewski et al. 2009). Therefore, other approaches to find the analytical solutions of the model need to be looked for.

Acknowledgments.

This work was done within the project "Mathematical models of fluid and solute transport in normal and pathological tissue" supported by Mianowski Fund (Warsaw, Poland). R.Ch. thanks the Department of Mathematical Modelling of Physiological Processes (IBIB of PAS, Warsaw), where the main part of this work was carried out, for hospitality.

References

[1] Bateman H (1974) Higher Transcentental Functions, Vol.2, Nauka, Moscow (In Russian)

[2] Cherniha R, Dutka V,Stachowska-Pietka J. and Waniewski J.(2007) Fluid transport in peritoneal dialysis: a mathematical model and numerical solutions. In: Mathematical Modeling of Biological Systems, Vol.I. Ed. by A.Deutsch et al., Birkhaeuser, pp.291-298

[3] Cherniha R, Waniewski J (2005) Exact solutions of a mathematical model for fluid transport in peritoneal dialysis. Ukrainian Math. J., **57**: 1112–1119

[4] Flessner MF (1994) Osmotic barrier of the parietal peritoneum. Am J Physiol 267:F861-870.

[5] Flessner, MF(2001) Transport of protein in the abdominal wall during intraperitoneal therapy. I. Theoretical approach. Am. J. Physiol. Gastrointest Liver Physiol., **281**: G424–437

[6] Flessner MF, Dedrick RL, Schultz JS (1984) A distributed model of peritoneal-plasma transport: theoretical considerations. Am J Physiol, 246:R597-607.

[7] Flessner MF, Fenstermacher JD, Dedrick RL, Blasberg RG (1985) A distributed model of peritoneal-plasma transport: tissue concentration gradients. Am J Physiol 248:F425-435.

[8] Gokal R and Nolph KD (1994) The textbook of peritoneal dialysis. Kluwer, Dordrecht.

[9] Imholz A.L., Koomen, G.C., Voorn, W.J., Struijk, D.G., Arisz, L., Krediet, R.T.(1998) Day-to-day variability of fluid and solute transport in upright and recumbent positions during CAPD. Nephrol. Dial. Transplant., **13** (1): 146–153

[10] Seames EL, Moncrief JW, Popovich RP (1990) A distributed model of fluid and mass transfer in peritoneal dialysis. Am J Physiol 258:R958-972.

[11] Stachowska-Pietka J, Waniewski J, Flessner MF, Lindholm B (2005) A mathematical model of peritoneal fluid absorption in tissue. Adv Perit Dial 21:9-12.

[12] Stachowska-Pietka J, Waniewski J, Flessner MF, Lindholm B (2006) Distributed model of peritoneal fluid absorption. Am J Physiol Heart Circ Physiol 291:H1862-1874.

[13] Stachowska-Pietka J, Waniewski J, Flessner MF, Lindholm B (2007) A distributed model of bidirectional protein transport during peritoneal fluid absorption. Adv Perit Dial 23:23-27.

[14] Waniewski, J. (2001) Physiological interpretation of solute transport parameters for peritoneal dialysis. J. Theor. Med., **3**, 177–190

[15] Waniewski J (2002) Distributed modeling of diffusive solute transport in peritoneal dialysis. Ann Biomed Eng 30:1181-1195.

[16] Waniewski J. (2004) A mathematical model of local stimulation of perfusion by vasoactive agent diffusing from tissue surface. Int. J. Cardiovas. Eng., **4**(1), 115–123

[17] Waniewski J (2008) Transit time, residence time, and the rate of approach to steady state for solute transport during peritoneal dialysis. Ann Biomed Eng36:1735-1743.

[18] Waniewski J, Dutka V, Stachowska-Pietka J, Cherniha R (2007) Distributed modeling of glucose-induced osmotic flow. Adv Perit Dial 23:2-6.

[19] Waniewski J, Stachowska-Pietka J, Flessner MF (2009) Distributed modeling of osmotically driven fluid transport in peritoneal dialysis: theoretical and computational investigations. Am J Physiol Heart Circ Physiol 296:H1960-1968.

[20] Waniewski J, Werynski A, Lindholm B (1999) Effect of blood perfusion on diffusive transport in peritoneal dialysis. Kidney Int 56:707-713.

[21] Zakaria E.R., Lofthouse J., Flessner M.F.(1999) In vivo effects of hydrostatic pressure on interstitium of abdominal wall muscle. Am. J. Physiol., **276**, H517–529